TU Delft

Interfacultair Reactor Instituut

IRI-131-92-021

CALIBRATION OF THE DODEWAARD DOWNCOMER THERMOCOUPLE CROSS-CORRELATION FLOW-RATE MEASUREMENTS

A.J.C. STEKELENBURG[†], T.H.J.J. VAN DER HAGEN[†] and H.E.A. VAN DEN AKKER[‡]

[†]Interfaculty Reactor Institute, Delft University of Technology, Mekelweg 15, 2629 JB Delft, The Netherlands
[‡]Kramers Laboratorium voor Fysische Technologie, Delft University of Technology, Prins Bernhardlaan 6, 2628 BW Delft, The Netherlands

December 1992

by order of *N.V. Gemeenschappelijke Kernenergiecentrale Nederland*

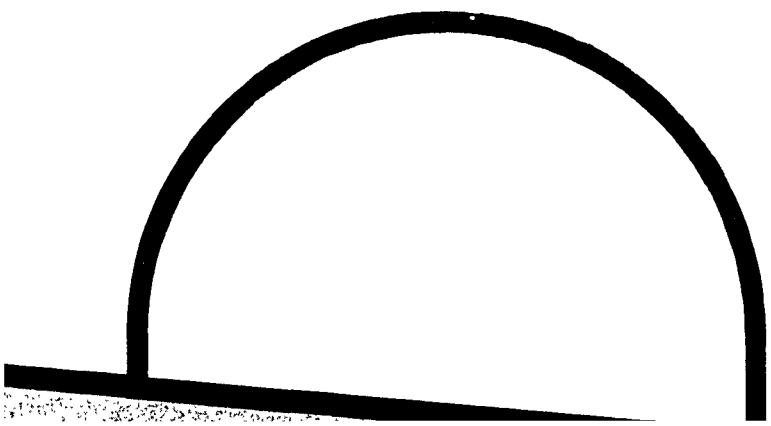

CALIBRATION OF THE DODEWAARD DOWNCOMER THERMOCOUPLE CROSS-CORRELATION FLOW-RATE MEASUREMENTS[§]

A.J.C. STEKELENBURG[†], T.H.J.J. VAN DER HAGEN[†] and H.E.A. VAN DEN AKKER[‡]

[†]Interfaculty Reactor Institute, Delft University of Technology, Mekelweg 15, 2629 JB Delft, The Netherlands

[‡]Kramers Laboratorium voor Fysische Technologie, Delft University of Technology, Prins Bernhardlaan 6, 2628 BW Delft, The Netherlands

[§]This report is an adapted version of:
A.J.C. Stekelenburg, T.H.J.J. van der Hagen, H.E.A. van den Akker, 'Numerical Simulation of Turbulent Flow for Calibration of Cross-Correlation Flow Measurements',
submitted for publication in the *International Journal of Numerical Methods for Heat and Fluid Flow*.

ABSTRACT

The cross-correlation flow measurement technique, applied for measuring the coolant flow rate in a nuclear reactor, was calibrated with the use of numerical simulations of turbulent flow. The three-dimensional domain was collapsed into two dimensions. With a two-dimensional calculation of steady-state flow with transient thermal characteristics the response of thermocouples to a temperature variation was calculated. By cross-correlating the calculated thermocouple responses, the link between total flow rate and measured transit times was made. Three calibration points were taken in the range of 579 kg/s to 1477 kg/s. In this range, the product of the calculated transit time and the mass flow-rate is constant up to +3.5 % and -2.4 %. The reliability of the calibration was estimated at ±4.6 %. The influence of the inlet boundary conditions, and the modelling of the flow in the upper part of the downcomer channel on the calibration result is shown to be small. A measured velocity profile effect was successfully predicted.

CONTENTS

INTRODUCTION

With the cross-correlation flow measurement technique, the average transit time of fluctuations in, for instance, the temperature from an upstream to a downstream detector is estimated[1]. This transit time supplies information on the flow velocity. A problem with the cross-correlation flow measurement technique is the interpretation of the measured transit time, and the conversion of this transit time into parameters like the average velocity or the mass flow rate, in particular in cases the flow field is not uniform. Usually this problem is solved by calibrating the technique with another flow meter. If no other flow meter can be installed, however, the measured transit time and the mass flow rate can be linked using information about the flow field through, for instance, numerical flow field calculations.

The latter strategy was applied to measuring the core coolant flow rate in the natural circulation cooled boiling water nuclear reactor at Dodewaard, The Netherlands (thermal power: 183 MW, operating pressure and corresponding saturation temperature: 75.5 bar and 291°C). The signals used for estimating the flow rate are noise signals of thermocouples which are located in the so-called downcomer channel (the area between the chimney and the core, and the reactor vessel wall, through which the circulating water flows downward - see *Figure 1* for reactor vessel cross-section). The noise signals of thermocouples which are only axially displaced and which are positioned in a region without too much flow disturbance show a high correlation, and a clear transit time phenomenon. As early as in 1969 these transit times were used for estimating local water velocities and the total coolant flow rate[2,3]. These measurements showed that the velocity varies over the downcomer channel. Thermocouple signals were simulated by combining fluid flow calculations and Monte Carlo simulations (see also Reference 3). With increased computer speed and capacity, improved computer programs, and improved analysis techniques it is possible to gain even more insight and make a reliable and accurate estimation of the flow rate[4].

Important ingredients of the translation of the noise signals to the flow rate are the characteristics of the downcomer flow field. In the current investigation this information is obtained by performing two- and three-dimensional turbulent flow calculations as well as simulation of steady state flow with transient thermal characteristics with the use of FLUENT[5,6], a general purpose computer program for modelling fluid flow. With this method the response of downcomer thermocouples to temperature fluctuations was directly simulated, thus providing a natural link between total flow rate and measured transit time.

Fundamentals of the computer program

The computer program FLUENT (V3.0) was used to calculate the characteristics of the downcomer flow field. With this program it is possible to model turbulence by two different turbulent flow models: a two-equation model (the k-ϵ model) or the Algebraic Stress Model. The equations for conservation of mass, momentum and energy are reduced to their finite volume analogues while the domain is divided into computational cells. The resulting set of equations is solved by a semi-implicit iterative scheme. Integration in time is fully implicit. For interpolation between grid points and for calculation of the derivatives of the flow variables a power law differencing scheme or a Quadratic Upwind Scheme (QUICK) is used. Different types of boundary conditions can be specified. For inlet cells velocity vectors and turbulence intensity must be specified. In symmetry cells zero gradient boundary conditions are applied (except for lateral

velocity components which must vanish). In outlet cells overall continuity is assured, and it is assumed that the flow is fully developed. The log-law of the wall is employed for computing wall shear stress in turbulent flow.

The geometry of the downcomer channel

The annular downcomer channel consists of two regions, an upper region surrounding the chimney, and a lower region next to the core (*Figures 1-3*). The shape of the chimney follows the arrangement of the outer fuel elements. The core is surrounded by the core shroud, which is a cylinder.

The downcomer channel is approximately 5.5 m in length. At the height of the chimney it is 0.4-0.5 m in width and in the lower region it is 0.338 m in width. The inner radius of the reactor vessel is 1.399 m.

An important obstruction in the downcomer channel is the feedwater sparger, which is a ring of 360°, and which has a height of 28 cm (in the flow direction) and a width of 10 cm. Cold feedwater is injected from tiny holes in the feedwater sparger into the downcomer channel. The feedwater flow is approximately 70 kg/s. The downcomer flow is approximately 1350 kg/s.

At each of two elevations, eight instrument support rings are mounted onto the inner wall of the vessel. These arched rings are stainless steel strips, 1 cm in thickness and 6 cm in height (in the flow direction) which follow the vessel wall over 41° at a spacing of 4 cm. This implies that the eight arcs do not cover 360° completely. These arcs, and the angularities of the chimney make the downcomer channel a three-dimensional problem.

The inner vessel wall is covered with stainless steel strips, leading to a corrugated wall with a roughness of approximately 2 mm and a period of 5 cm.

Downcomer thermocouples and temperature noise

The thermocouples are installed at different heights (coded 1-5), at different penetrations into the flow (coded A and B), and at different angular positions in the downcomer channel (coded X, Y, and Z - see *Figures 1* and *2*). Furthermore, at all positions two thermocouples are installed with 5 cm axial displacement (coded 1 and 2). The signals of these short distance thermocouple pairs show high correlation, but because of the short distance there is a relatively large influence of the velocity profile depression caused by the instrument tube the thermocouples are mounted on. Regarding the large distance thermocouple pairs, the fluctuations will be carried by the bulk of the flow, and the effect of the profile depression may be negligible. Of these large distance thermocouple pairs, only the pairs of thermocouples next to the core (elevations 4 and 5) do show high correlation and a clear transit time phenomenon, due to the disturbance of the flow in the vicinity of other thermocouples. Presently, of these 4 and 5 elevation thermocouples only thermocouples A41Y and A52Y can be used.

The RMS-value of the inherent temperature fluctuations is approximately 0.5°C (the average temperature is 285°C at the operating pressure of 75.5 bar), and 90 % of the noise power contribution originates from frequencies below 0.5 Hz. From the combination of this value with a flow velocity of 0.8 m/s it follows that the temperature fluctuations wave length is over 1.6 m.

THREE-DIMENSIONAL CALCULATIONS

As described above, the annular downcomer channel represents a three-dimensional problem. Arguments as to symmetry make that the calculation domain can be limited to a segment of 45°. Because of the size of the domain and the flow conditions (the Reynolds number is approximately 4×10^6), the three-dimensional grid, having a maximum of 25,000 grid cells, will be too coarse, which will lead to lower reliability of the calculational result. The reliability of the result can be investigated by performing test calculations in which the influence of grid cell size, discretization scheme and turbulence model on the calculational result is investigated. These calculations demonstrate, as shown below, that the three-dimensional problem may confidently be collapsed into a typical two-dimensional plane in which much smaller grid cells can be applied.

The annular downcomer channel is modelled in cylindrical coordinates. Following the convention of computational fluid dynamics, the flow direction, which is downward in this case, is called the x-direction, the radial coordinate is called y, and the angle is called z. The corresponding velocities are called u, v, and w, respectively.

Set-up

For the annular downcomer channel, a three-dimensional grid of $x \times y \times z = 59 \times 21 \times 20 = 24{,}780$ cells was designed. Where large changes in flow field quantities were expected the grid cells were taken smaller. Inlet cells were put in the first x-plane, outlet cells at the last x-plane, and symmetry cells at the first and last z-plane. The last y-plane was completely filled with wall cells. The first 5 y-planes were filled in such a way that the shape of the chimney was approximated. The result of the geometric modelling is plotted in *Figure 3*.

Because the support rings are smaller (1 cm in y-direction) than the grid cells at that location (2.5 cm), the rings were modelled with the use of FLUENT's porous media option. With this option a pressure drop per unit length of $\frac{1}{2}C\rho u^2$, where ρ is the water density and C (m^{-1}) is a constant, is introduced over the grid cell. The constant C is obtained from the drag coefficient C_w for flow around objects. With a C_w of 2 for square rods and a length of the strip of 6 cm, C is $2/(0.06\ m) = 33\ m^{-1}$.

A uniform velocity and turbulence intensity distribution was taken at the inlet cells. The turbulence intensity was taken the program's default value of 10 %.

The physical properties of water at 75.5 bar and 285°C (operating conditions) given in *Table 1* were used[7].

Reliability

The reliability of the three-dimensional calculation was checked by performing test calculations for a small part of the downcomer channel. The test domain was taken two-dimensional in annular geometry. With this domain it was possible to reduce the mesh size with a factor of four in each direction. Also, the model for turbulence, and the discretization scheme were varied.

Because for this application the transport of temperature fluctuations is important, the reliability of the calculation was judged by looking at the calculated u-velocity at several positions. It was found that the difference between the calculated u-velocities for various settings was sometimes as large as 20 % at some positions.

This result demonstrated the necessity for applying a finer mesh. Because the maximum number

Table 1 Data on the downcomer flow

physical quantity	unit	actual value above sparger	actual value below sparger	value in 3D calculation	value in 2D calculation
flow surface at sparger level	m^2	3.52	-	3.53	3.75
temperature	°C	290	285	285	277*
density	kg m^{-3}	732	743	743	743
dynamic viscosity	kg m^{-1} s^{-1}	$8.96x10^{-5}$	$9.17x10^{-5}$	$9.17x10^{-5}$	$9.17x10^{-5}$
thermal conductivity	W m^{-1} K^{-1}	0.568	0.577	-	0.577
specific heat capacity	J kg^{-1} K^{-1}	$5.50x10^3$	$5.35x10^3$	-	$5.35x10^3$

*The temperature is varied in time (see *Figure 9*), 277°C is the inlet temperature at the beginning of the simulation and the inlet temperature after 2 s.

of grid cells was used already it was investigated whether the calculation domain could be two- rather than three-dimensional. This was done by looking at the angular dependence of the axial flow calculated with the three-dimensional domain. The flow rate in the x-direction through all grid cells (all possible y-positions) at a certain x- and z-position was summed. This was done for all angles and for three elevations: at the top of the core, and at thermocouple elevations 4 and 5. The result is plotted in *Figure 4*. This plot shows that the flow varies some 10 % with angular position.

However, at 150° (the Y-thermocouple plane) the difference between the mass flux at thermocouple elevations 4 and 5 is only 0.5 %. From this it can be concluded that the three-dimensional domain can confidently be collapsed into two dimensions. The magnitude of the flow rate applied in the two-dimensional calculation and the flow rate in reality can be linked with the use of the angular dependence shown in *Figure 4*.

This result was obtained from the three-dimensional calculation which was found to lead to erroneous results. The reliability of the angular dependence (which is an integrated quantity) following from this calculation, was investigated by performing calculations for a smaller, but still three-dimensional domain. This domain (*Figure 5*) was a part of the downcomer channel next to the core which included an instrument support ring. The domain was limited to 30° and the length was 83 cm. This offered the possibility of reducing the grid cell size with a factor of two in all directions. With the coarse grid the support ring was modelled with porous cells. With the fine grid the cells were small enough to allow for modelling the strip by wall cells. As in the two-dimensional test calculation, the model for turbulence and the discretization scheme were varied. Also, the influence of wall roughness and inlet turbulence intensity was studied. The calculation results were judged by looking at the summation of the calculated flow rate of all cells at the outlet at the z-plane the thermocouples are located. For all test calculations the difference between the result and the average of all tests was smaller than 0.3 %. From this it can be concluded that although the calculated u-velocity is strongly dependent on grid size, turbulence model, and discretization scheme, the angular dependence of the flow rate (*Figure 4*) can be reliably calculated

from the three-dimensional calculation.

Results

From the three-dimensional calculation for the full geometry (*Figure 3*) it followed that the flow at the Y-thermocouple angular position (150°) is mainly two-dimensional. For linking the flow rate in a two-dimensional calculation and the flow rate in reality, the mass flux at the Y-thermocouple angular position is important. Quantitatively, this link can be expressed in terms of the calculated mass flux ϕ''_c at this angular position, as compared to the mass flux ϕ''_u following from an angularly uniform flow distribution, by introducing a form factor f

$$f = \frac{\phi''_c}{\phi''_u}. \qquad (1)$$

For ϕ''_c the average value of the mass fluxes in the thermocouple plane at thermocouple elevations 4 and 5 can be taken. In a calculation with a total flow rate of 1500 kg/s, the calculated mass flux at the thermocouple plane was found to be 563.6 kg m^{-2} s^{-1}, while ϕ''_u = 573.5 kg m^{-2} s^{-1}, leading to f=0.9827. From this value it follows that the calculated mass flux is 1.7 % lower than in the uniform case.

In order to check whether this result is applicable to a wide range of flow rates, another three-dimensional calculation was performed with a total flow rate of 600 kg/s. The mass flux at the thermocouple plane following from this calculation was 225.6 kg m^{-2} s^{-1}, while in the uniform case the mass flux would be 229.4 kg m^{-2} s^{-1}. From these values it follows that f=0.9834 and that also at this flow rate the calculated mass flux is 1.7 % lower than in the uniform case.

These two calculations show that the value f=0.983 can be used to collapse the three-dimensional domain into two dimensions.

It was stated above (see *Reliability*) that all three-dimensional test calculations lead to the same result for the mass flux within ±0.3 %. Because the downcomer channel includes two axially displaced support rings (*Figure 3*), and the test calculation domain only one (*Figure 5*), this value can be multiplied with a factor of two when applied to the full geometry. The resulting value of ±0.6 % can be used for the 95 % confidence interval for the calculated form factor f, leading to f=0.983±0.006. Of course it must be remarked that the estimation of the error follows from a comparison of calculation results only rather than from a comparison with measurements.

TWO-DIMENSIONAL CALCULATIONS

By calculating the problem in two dimensions (in annular geometry), a much finer grid can be applied within the limit of 25,000 grid cells. The form factor, as introduced above, can be used to link the total (three-dimensional) flow rate to the flow rate that is applied in the two-dimensional calculation.

With a calculated velocity vector field however, the problem has not been solved yet. The purpose of the investigation was to establish a link between the total flow rate and the measured transit time between thermocouple signals. This translation is made by performing a simulation of the advection of a temperature fluctuation.

Steady-state flow

Feedwater is injected with a velocity of approximately 7 m/s from tiny holes in the feedwater sparger into the downcomer flow in the +y and -y direction. This will lead to a perturbation of the downcomer flow. This process is modelled in two dimensions (in annular geometry) by representing the sparger with the individual holes by sparger with a ring (in three dimensions) from which water flows. The effect of the water injection from the ring on the downcomer flow was approximated by equating the momentum flow rate of the injected feedwater in model and reality; hence,

$$\phi_f + \phi_c = c_1 \tag{2}$$

$$\frac{\phi_f |v|_f}{\phi_c |v|_c} = c_2, \tag{3}$$

where ϕ and v are the flow rates and velocities respectively, the subscripts f and c denote feedwater and circulating water respectively, and the constants c_1 and c_2 should be equal in model and reality. With this modelling, it can be taken into account that the outflow area of the ring is not equal to the area of the holes. The problem that the number of holes is different for the inside and the outside of the feedwater sparger is solved by applying (2) and (3) to the inside and the outside separately. Finally, the flow from the outside holes is deflected in the +z, -z and +x-direction by deflectors on the feedwater sparger. This is modelled by calculating the feedwater flow rate and velocity with (2) and (3), and rotating the inlet velocity vector 45° into the x-direction, leading to equal components in the x and y-direction, and a reduction of the flow rate with a factor of $\sqrt{2}$.

The domain of the two-dimensional calculation is plotted in *Figure 6*. The length of the domain is the same as in the three-dimensional calculation. Also, the thickness of the downcomer channel next to the core is the same. For the thickness next to the chimney, the actual distance between the vessel wall and the chimney at the Y-thermocouple angular position was taken. The calculation was performed in annular geometry. A grid of $268 \times 93 = 24.924$ cells was designed. As in the three-dimensional calculation the grid cells were taken smaller where large changes in flow field variables were expected. Grid cell size allowed for modelling the instrument support rings by a set of wall cells. As in the three-dimensional calculation inlet cells were taken in the first x-plane, and outlet cells in the last x-plane. Two additional inlet cells were placed in the sparger for modelling of feedwater injection. These cells had a length (in the x-direction) of 6.2 mm.

In order to calibrate the flow measurement technique over a large range of the flow rate, several cases were calculated (see *Table 2*, cases A, B, and C). The sensitivity of the technique to the modelling of the feedwater flow was tested by considering a case for which the total flow rate was the same as in case A, but for which the feedwater flow rate was halved (case D). The model flow rates given in *Table 2* were calculated from the actual flow rates by applying (2) and (3) with the use of the values given in *Tables 1* and *3*, and the form factor $f = 0.983$. In *Figure 7* the calculated stream lines for case A are plotted for the region near the feedwater sparger. The plot shows that the feedwater injection strongly influences the downcomer flow field. In *Figure 8* the calculated profiles of the u-velocity for the same case are plotted for the lower region next to the

core. It can be seen that the u-velocity profile changes downstream, which explains qualitatively that using different thermocouple pairs leads to different measured u-velocities[2,3].

Table 2 The two-dimensional calculation cases A-D

case	actual total flow (kg/s)	actual feedwater flow (kg/s)	total flow in 2D (kg/s)	inside feedwater flow (kg/s)	outside feedwater flow (kg/s)	transit time (s)	product of transit time and total flow (10^3 kg)
A	1477	80	1453	99	55	1.96	2.89
B	1078	80	1060	97	54	2.72	2.93
C	579	80	570	90	50	5.29	3.06
D	1477	40	1453	50	27	1.99	2.94

Table 3 Data on the feedwater flow

physical quantity	unit	actual value	value in 2D calculation
surface at inside of sparger	m^2	7.96×10^{-3}	46.3×10^{-3}
surface at outside of sparger	m^2	4.51×10^{-3}	50.2×10^{-3}
temperature	°C	138	277
density	kg m^{-3}	932	743
dynamic viscosity	kg m^{-1} s^{-1}	2.01×10^{-4}	9.17×10^{-5}
thermal conductivity	W m^{-1} K^{-1}	0.697	0.577
specific heat capacity	J kg^{-1} K^{-1}	4.26×10^{3}	5.35×10^{3}

Simulation of transient flow

The advection of water temperature fluctuations was simulated by varying the inlet temperature in time and calculating the temperature field under transient thermal conditions. The inlet temperature introduced as a function of time is plotted in *Figure 9*. By choosing this triangular shape the power spectral density of the applied fluctuation is non-zero up to 1 Hz. The fluctuation was applied uniformly over the inlet cells. During simulation the temperature at the thermocouple locations was registered as a function of time. In this way, the response of the thermocouples to a temperature fluctuation at the inlet was directly simulated. As only the advection of the temperature fluctuation is important here, heat sources like the hot core, or heat sinks like the vessel wall were not taken into account - the heat flux density through all walls was taken zero. For the same reason the feedwater temperature was taken constant in time at a value of 550 K.

The integration in time is treated fully implicitly, which implies that the time step for

performing the time simulation is not limited by the *Courant-Friedrichs-Lewy stability condition* for explicit discretization of a hyperbolic equation (see, for instance, Reference 8). Accuracy, however, is of course influenced by the choice of the time step. The time step was chosen such that, for most grid cells the product of the time step and the u-velocity is smaller than the length of the cell.

The reliability of the transient flow simulation was tested with the use of a smaller two-dimensional domain. During this simulation, the inlet temperature was varied as a function of time as plotted in *Figure 9*, and the temperature at the outlet, 8 cm from the vessel wall (corresponding to a thermocouple position) was registered. The time position of the maximum registered temperature was determined for different mesh sizes, time steps, turbulence models, turbulence intensities, discretization schemes, convergence criteria, wall roughness, and inlet temperature fluctuation amplitude and temperature offset. For reasonable values of the above mentioned variables the time position of the maximum was always located in an interval of ± 2.3 % around the average value. Variation of the time step did affect the registered temperature - a larger time step resulted in a spread of the temperature fluctuation - but did not affect the time position of the maximum temperature.

Turning back to the simulation of transient flow for the two-dimensional downcomer channel, in *Figure 10* the contours of the temperature function for case A for consecutive moments in time for different regions of this channel are plotted. It can be seen from the figure how the temperature fluctuation is transported downwards by the flow. In *Figure 11* the calculated temperature resonse of the two thermocouples A41Y and A52Y was plotted. From this plot the delay of temperature signal of A52Y, which is a downstream thermocouple, with respect to the signal of A41Y can be clearly seen. Also, for instance from the maximum value of the temperature, it can be seen that the temperature fluctuation is attenuated.

Validation

The transit times between the calculated thermocouple responses to the applied temperature perturbation are estimated with the use of the usual cross-correlation techniques[1]. Because the mass flow rate is an unknown variable in the measurements, the absolute values of the transit times obtained by measurements cannot be compared with the transit times following from the calculation. However, measured velocity profile effects, i.e. the relative differences between velocities measured with thermocouple pairs at different radial positions, can be compared with the values following from the calculations.

As already mentioned above, only the large distance thermocouple pairs in the lower region of the downcomer channel (see *Figure 2b*) are reliable for velocity estimation. For these large distance thermocouple pairs, the calculations for case A show that the velocity derived from the transit time between signals of the thermocouples 16 cm from the vessel wall is 92.7 % of the velocity obtained from the thermocouples 8 cm from the vessel wall. This prediction is in good agreement with measurements performed by Termaat[2] who found that the velocity derived from the transit time measured with the thermocouples 16 cm from the wall is 93.8 % of the velocity measured with the thermocouples 8 cm from the wall.

The fact that the velocities measured with small distance thermocouple pairs are strongly affected by the profile depression caused by the thermocouple instrument tube itself is illustrated

by applying the same analysis to the small distance pairs. For instance, from the measurements by Termaat it follows that the velocity measured with the lowest pair of thermocouples 8 cm from the wall is 75.4 % of the velocity measured with the large distance thermocouples 8 cm from the wall. From the calculations, however, in which the instrument tubes were not modelled, it follows that both velocities should be the same. From this result it can be concluded that the profile depression is as large as 25 % for the small distance thermocouple pairs.

SYNTHESIS OF TWO- AND THREE-DIMENSIONAL CALCULATIONS

The results for the transit time between thermocouple signals A41Y and A52Y for cases A-D are given in *Table 2*. Also, in this table the product of the transit time and the mass flow rate is given. This quantity shows that the transit time is inversely proportional to the mass flow rate within +3.6 % and -2.2 % for all four cases. The deviation is systematic - a higher flow rate leads to a larger product of flow rate and transit time. The result is presented graphically in *Figure 12*. In this figure the inverse of the transit time is plotted as a function of the mass flow rate. This plot can be considered as the calibration curve for the cross-correlation flow rate measurements.

In *Figure 12* and *Table 2* it can also be seen that the results of the cases A and D differ by 2 % only, although the feedwater flow rate in case A is twice the value in case D. From this it can be concluded that although the injection of feedwater strongly affects the downcomer flow (see *Figure 7*), the transit time between the thermocouples A41Y an A52Y is hardly influenced by the amount of feedwater which is injected. This implies that possible errors in the modelling of the flow in the upper part of the downcomer channel only have a small influence on the calculated transit time.

The reliability of the calibration technique can be estimated, once all sources of errors have been considered. As treated above, the comparison of results of three-dimensional test calculations leads to a relative error of ± 0.6 % in the form factor f. From the investigation concerning the reliability of the two-dimensional transient flow simulations treated above, it was found that for a smaller domain (83 cm length) the error did not exceed ± 2.3 %. As the distance between the thermocouples A41Y and A52Y is 1.6 m, ± 4.6 % can be taken as the error interval. Combining the estimated errors for the two- and three-dimensional calculations and assuming that the errors are independent, the error interval of the calibration technique can be taken ± 4.6 %. Again it must be stressed that the estimated errors follow from the comparison of the results of many test calculations, and that indeed it is still possible that all calculations deviate systematically from reality.

USING THE CALIBRATION CURVE IN PRACTICE

Application at 75.5 bar and 285 °C

The calibration method applied here involved calculating the transit time τ, starting from a given mass flow-rate ϕ. When interpreting a measured transit time, the mass flow-rate can be estimated by graphically interpolating *Figure 13*, which is the inverse of *Figure 12*, or it can be calculated by using the data given in *Table 2*. For the range of transit times from 1.96 s to 5.29 s, three calibration points are given. In absence of a theoretical model, and only a small non-linearity, it is sufficient to linearly interpolate between the given values of the product of mass flow-rate and transit time, to find the value corresponding with the measured transit time. The resulting value divided by the measured transit time is the estimation of the mass flow-rate.

Example:
measured transit time: 2.11 s →
interpolate between $\tau\phi = 2.89 \times 10^3$ kg ($\tau = 1.96$ s) and $\tau\phi = 2.93 \times 10^3$ kg ($\tau = 2.72$ s) →
take $\tau\phi = 2.90 \times 10^3$ kg →
result: $\phi = 1.37 \times 10^3$ kg/s.

Application at other operating conditions

System pressure and temperature affect the physical properties of water, which in turn results in a different flow field. For example, changing the operating condition from 75.5 bar and 285°C to 25 bar and 220°C leads to a change in the Reynolds number of 20 %. The largest effect of this change is expected to occur in the region near the wall. As this region is very small, the effect on the flow field of the bulk of the flow will also be small. As no calculations were performed at operating conditions other than 75.5 bar and 285°C, no estimation of the magnitude of the effect can be given.

If it is assumed that the effect of pressure and temperature on the flow field is small, not the product of the mass flow-rate and the transit time is important, but the product of the volumetric flow-rate and the transit time. To obtain this quantitity, the product listed in *Table 2* must be divided by the density at 75.5 bar and 285°C, which is taken 743 kg/m³. The correct product of the mass flow-rate and the transit time is obtained by multiplying by the density at the different operating condition.

Example:
at 60 bar and 270°C: measured transit time: 2.34 s →
$\tau\phi$ at 75.5 bar and 285°C:
interpolate between $\tau\phi = 2.89 \times 10^3$ kg ($\tau = 1.96$ s) and $\tau\phi = 2.93 \times 10^3$ kg ($\tau = 2.72$ s) →
take $\tau\phi = 2.91 \times 10^3$ kg.
divide $\tau\phi$ by the density at 75.5 bar and 285°C (743 kg/m³) and multiply by the density at 60 bar and 270°C (768 kg/m³) → $(\tau\phi)' = 3.01 \times 10^3$ kg →
result: $\phi = 1.29 \times 10^3$ kg/s.

Error estimation

For an estimation of the error in the estimation of the mass flow-rate, the statistical error in the transit time measurement and the error in the calibration procedure have to be combined. Because the two sources of error are independent, the errors can be quadratically summed. For a series of measurements with only a small range of transit times, the error in the calibration procedure is the same for all measurements. In this case, the total error consists of a statistical error from the transit time measurement, and a systematic error from the calibration procedure.

CONCLUSIONS

The thermocouple signal cross-correlation flow measurement technique was calibrated by performing numerical fluid flow simulations. The method is applied to the measurement of the core coolant flow rate of a nuclear reactor. The procedure comprises a combination of the extensive use of the computer code's modelling possibilities, including steady-state as well as

transient flow, powerful calculational data processing and interpretation, and many test calculations.

The calculated flow field following from a coarse-grid three-dimensional calculation was used to confidently collapse the three-dimensional geometry into two dimensions, although the calculated u-velocity showed a large dependence on grid cell size, discretization scheme and turbulence model.

With a fine-grid two-dimensional calculation the propagation of a temperature fluctuation was simulated. By registering the temperature resonse at the thermocouple positions, and applying cross-correlation techniques, the relationship between the measured transit time and the flow rate was established. Three calibration points were taken in the range of 579 kg/s to 1477 kg/s. In this range, the product of the calculated transit time and the mass flow-rate is constant up to +3.5 % and -2.4 %. The influence of the inlet boundary conditions, and the modelling of the flow in the upper part of the downcomer channel on the calibration result is shown to be small. By combining the results of various test calculations, the overall error of the calibration technique was estimated at $\pm$4.6 %.

Comparison of the transit times following from the calculations and measured transit times shows that the effect of a radial u-velocity profile can be successfully predicted.

REFERENCES

1. M.S. Beck and A. Pląskowski, Cross Correlation Flowmeters - their Design and Application, Adam Hilger, Bristol, 1987
2. K.P. Termaat, 'Fluid flow measurements inside the reactor vessel of the 50 MWe Dodewaard nuclear power plant by cross-correlation of thermocouple signals', J.Phys.E:Sci.Instrum. **3**, 589-593 (1970)
3. W.J. Oosterkamp, 'Reactor physics at the Dodewaard reactor', KEMA Scientific & Technical Reports **5**, 219-257, Arnhem, The Netherlands, 1987
4. A.J.C. Stekelenburg, T.H.J.J. van der Hagen and W.H.M. Nissen, 'The downcomer flow in a natural circulation cooled BWR', proceedings of SMORN VI - A symposium on nuclear reactor surveillance and diagnostics (ed. R.C. Kryter and B.R. Upadhyaya) May 19-24, 1991, Gatlinburg, Tennessee, U.S.A., **1**, 37.01-37.12, Oak Ridge National Laboratory / The University of Tennessee, Knoxville, 1991
5. FLUENT User's Manual 1990, creare.x Incorporated, Hanover
6. G.W. Colenbrander, 'CFD in research for the petrochemical industry', Applied Scientific Research **48**, 211-245 (1991). R.V.A. Oliemans (ed.). Computational Fluid Dynamics for the Petrochemical Process Industry, 1-35, Kluwer Academic Publishers, The Netherlands, 1991
7. R. Suessbrich, H2O computer program (based on VDI steam tables and other improved publications), Uhde GmbH, Dortmund (1978)
8. R. Peyret, and T.D. Taylor, Computational Methods for Fluid Flow, Springer Verlag, New York, 1983

LIST OF FIGURES

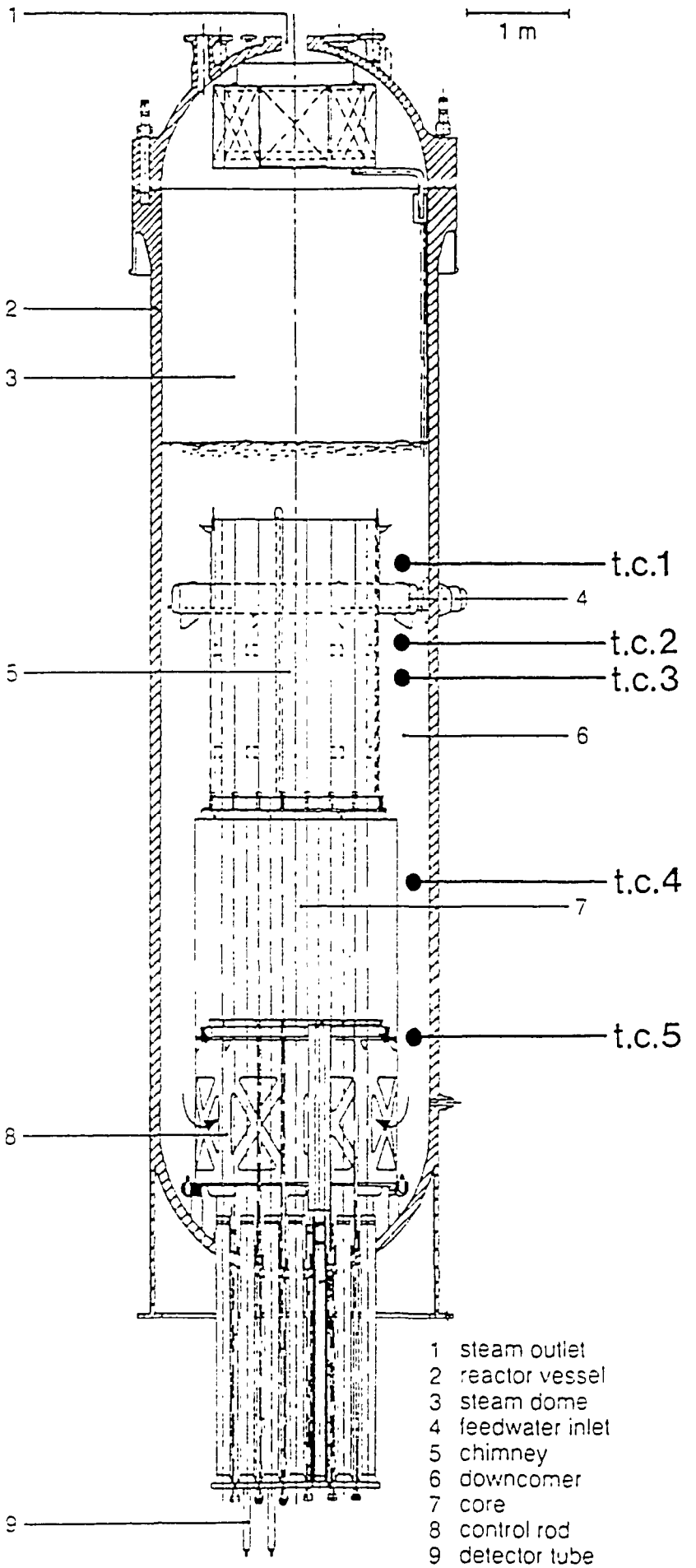
1 m
t.c.1
t.c.2
t.c.3
t.c.4
t.c.5
1 steam outlet
2 reactor vessel
3 steam dome
4 feedwater inlet
5 chimney
6 downcomer
7 core
8 control rod
9 detector tube

Figure 1

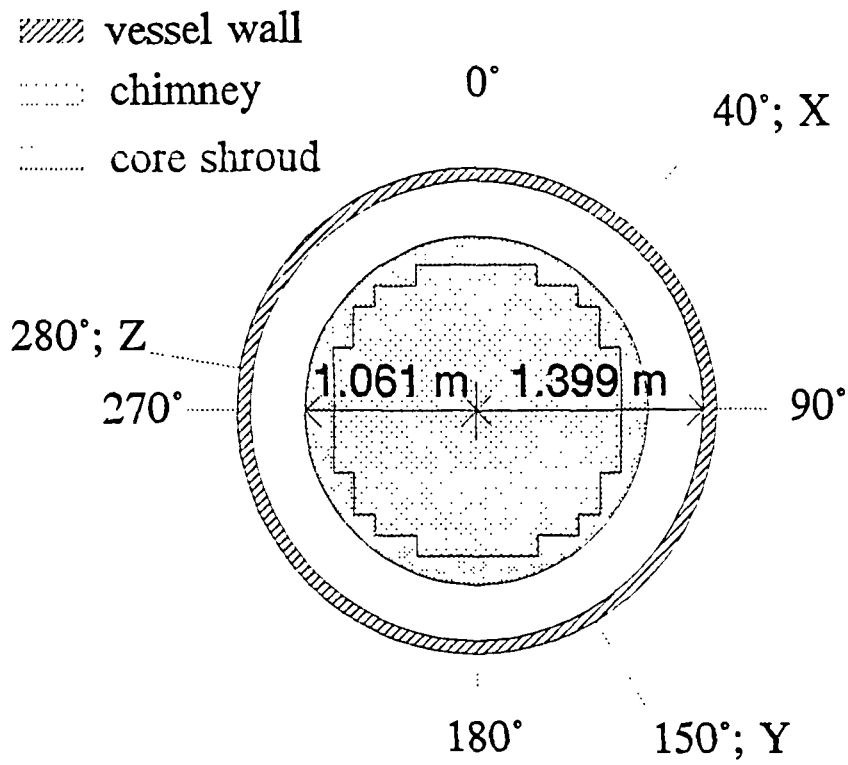

Figure 2a

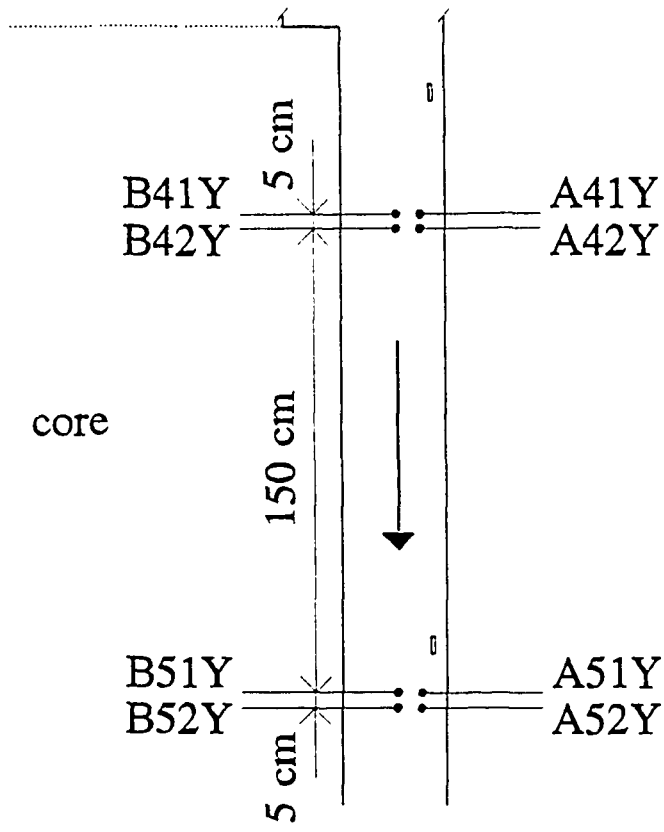

Figure 2b

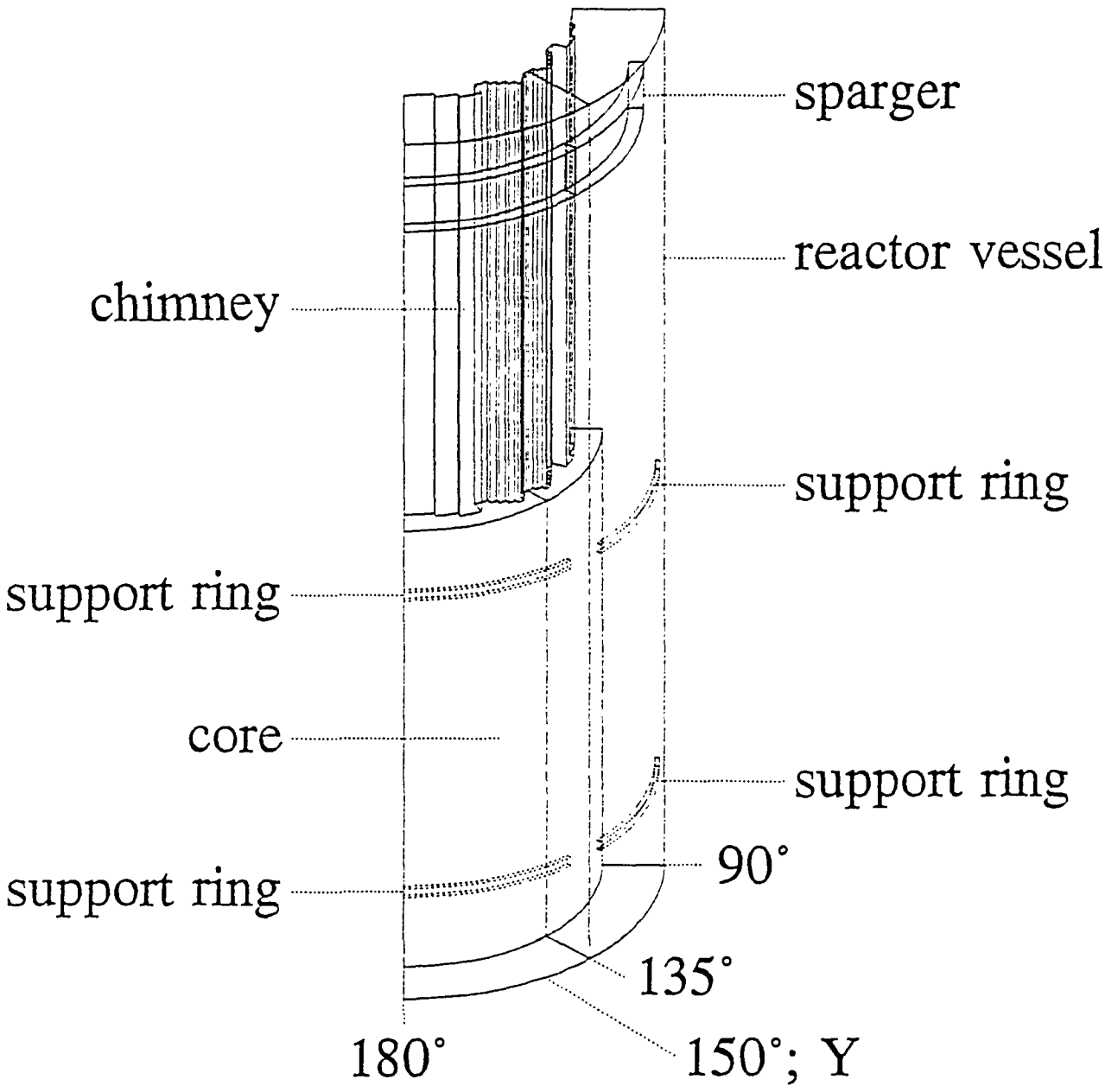
sparger
reactor vessel
chimney
support ring
support ring
core
support ring
support ring
90°
135°
180°
150°; Y

Figure 3

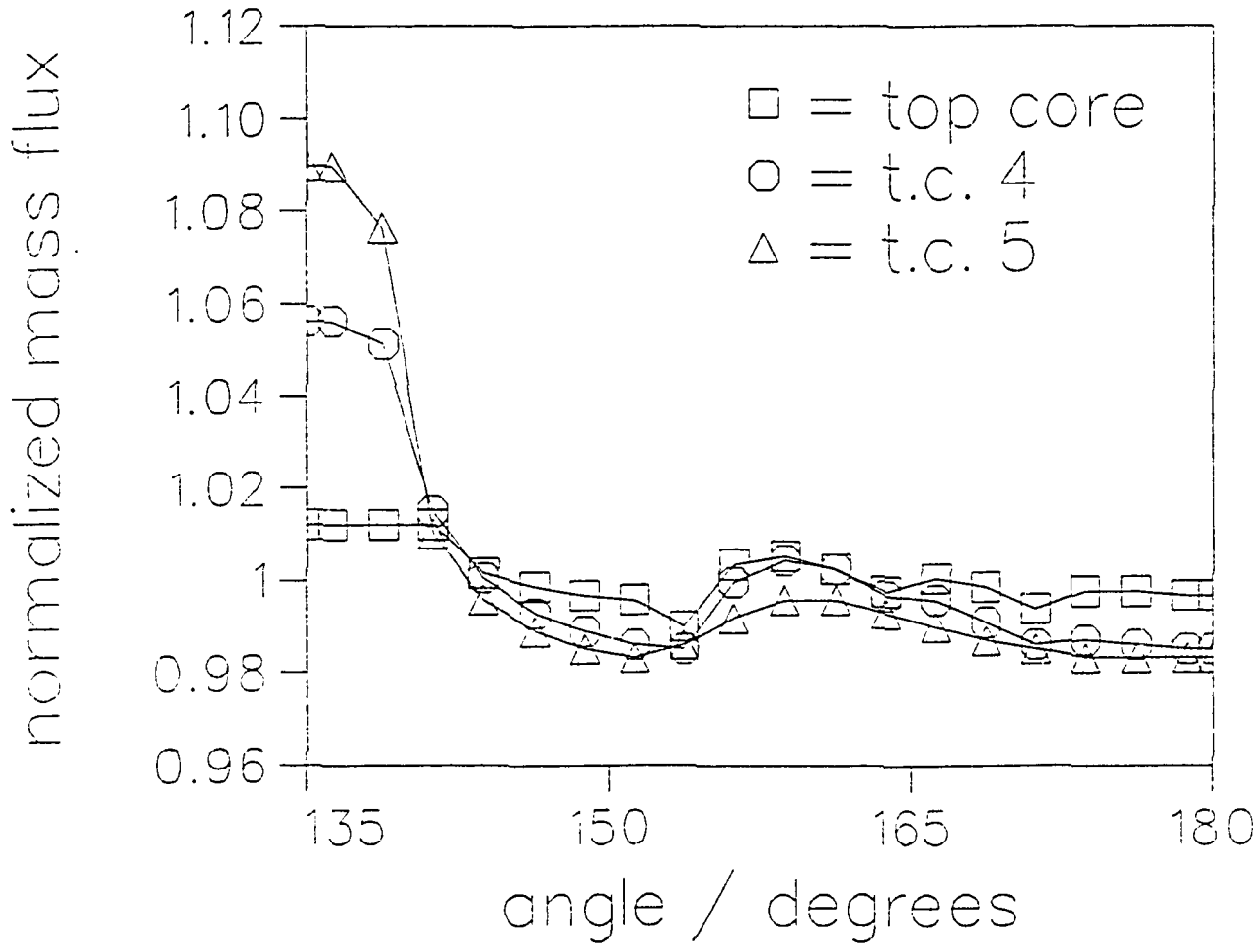
normalized mass flux
1.12
1.10
1.08
1.06
1.04
1.02
1
0.98
0.96
135
150
165
180
angle / degrees
□ = top core
○ = t.c. 4
△ = t.c. 5

Figure 4

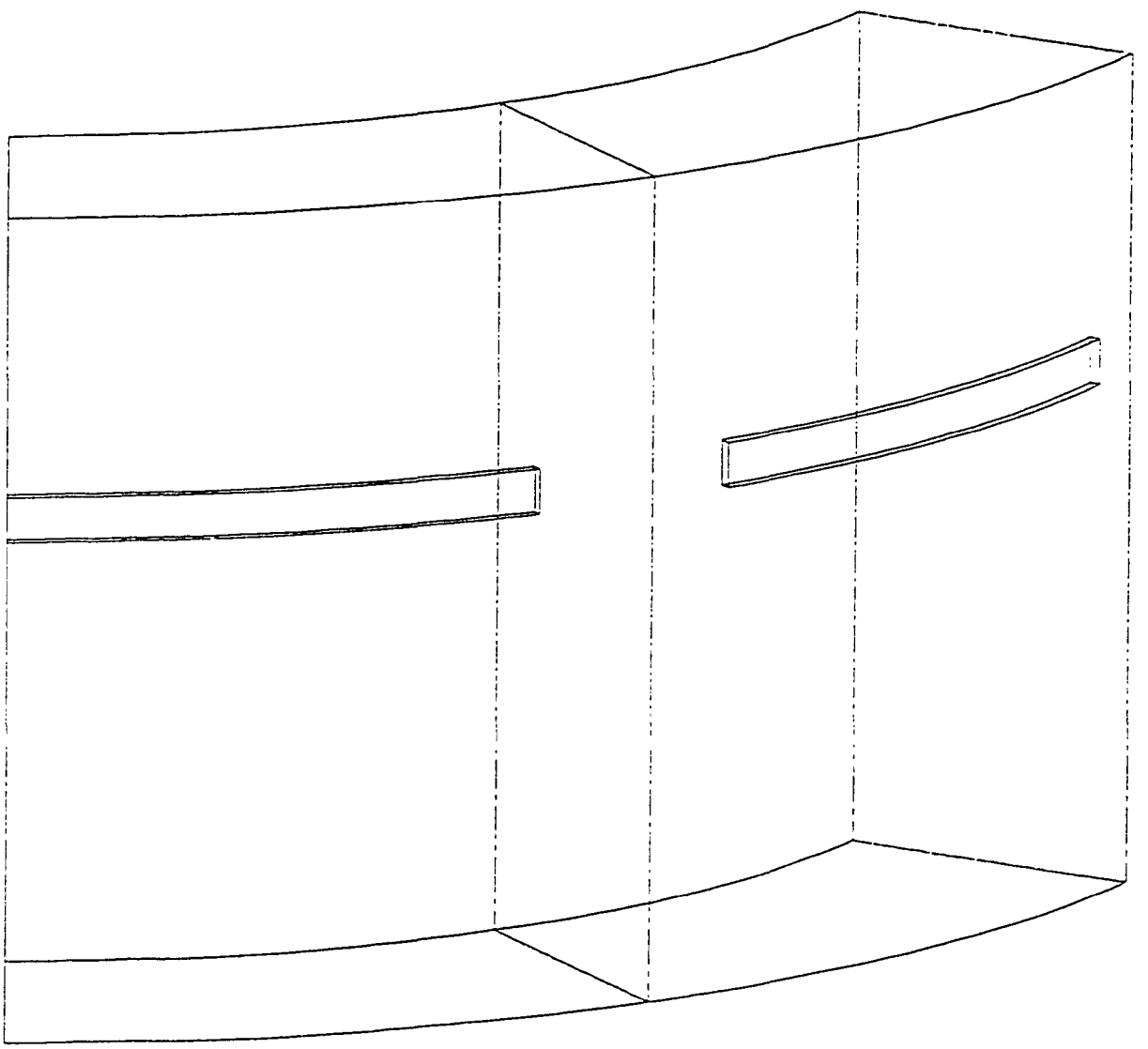

Figure 5

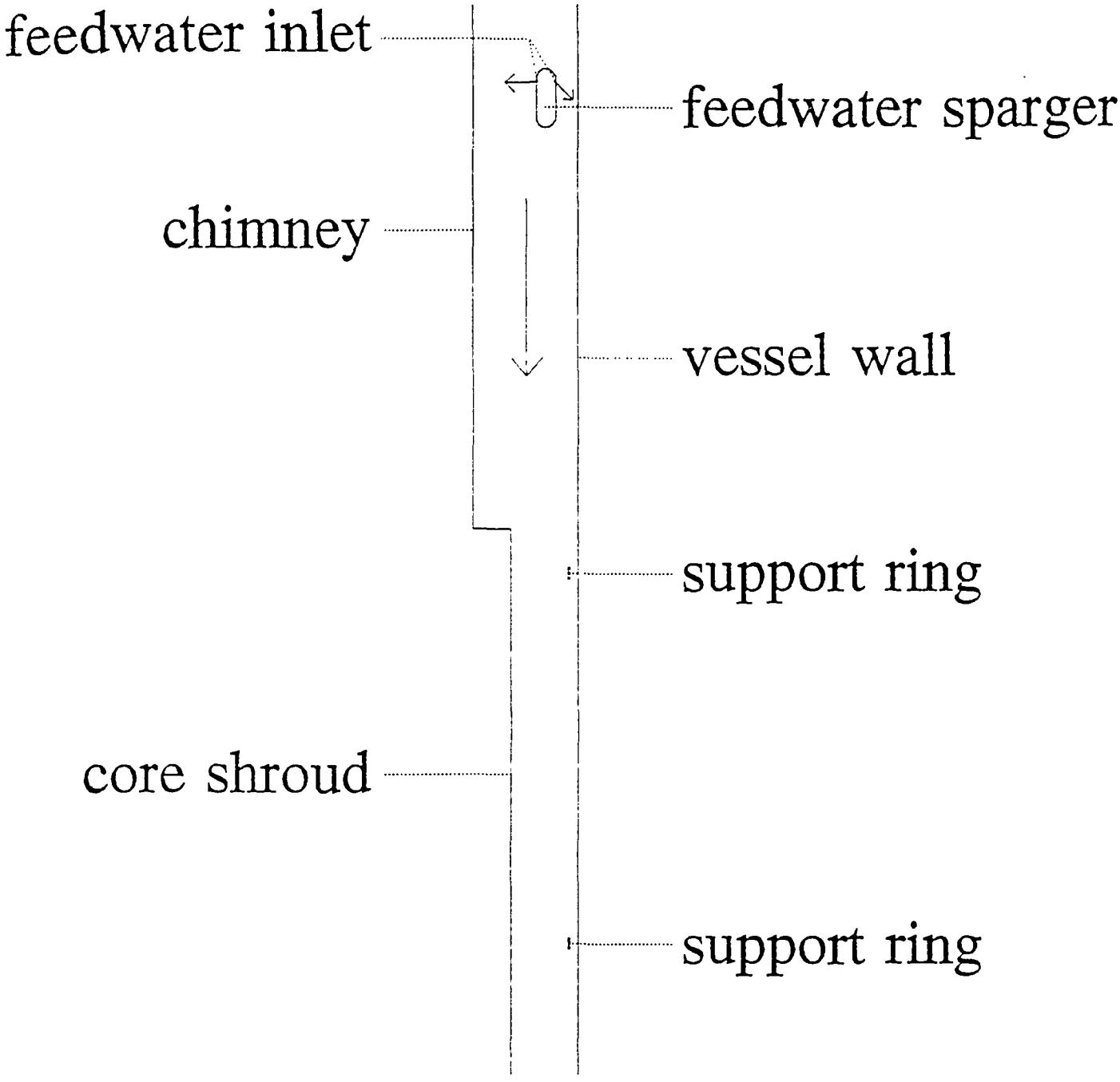
feedwater inlet
feedwater sparger
chimney
vessel wall
support ring
core shroud
support ring

Figure 6

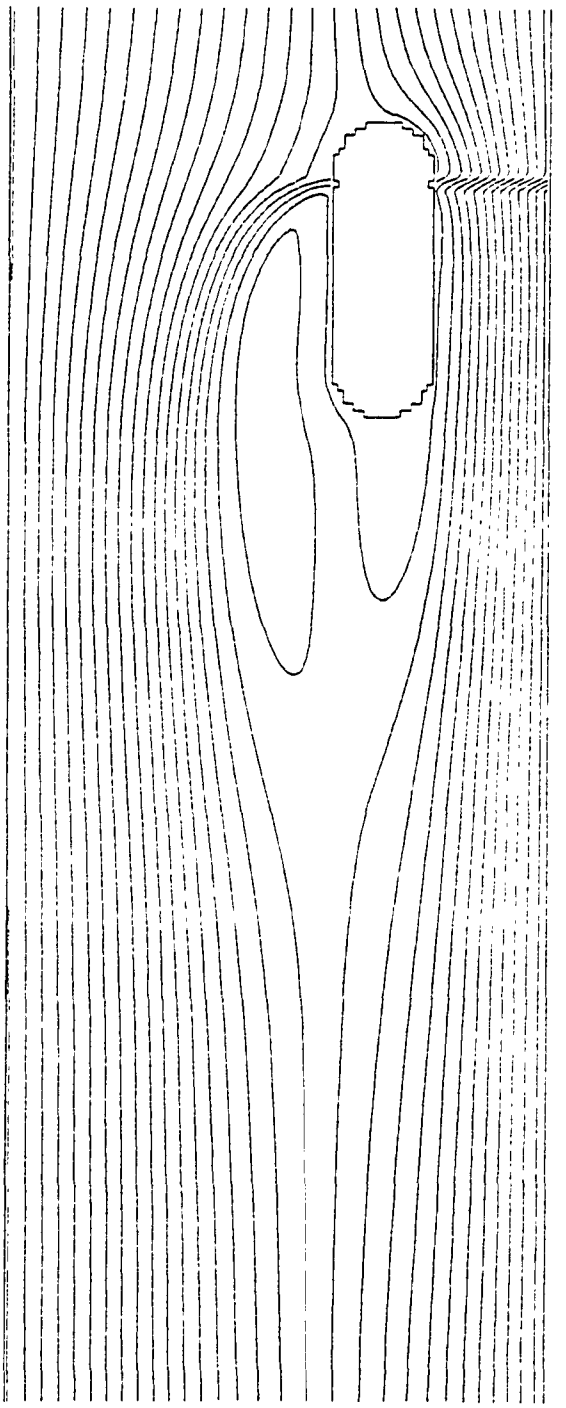

Figure 7

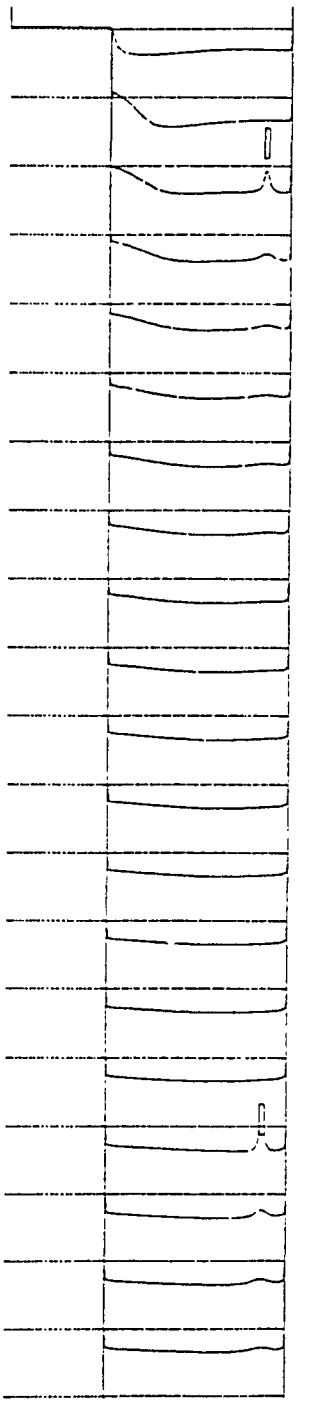

Figure 8

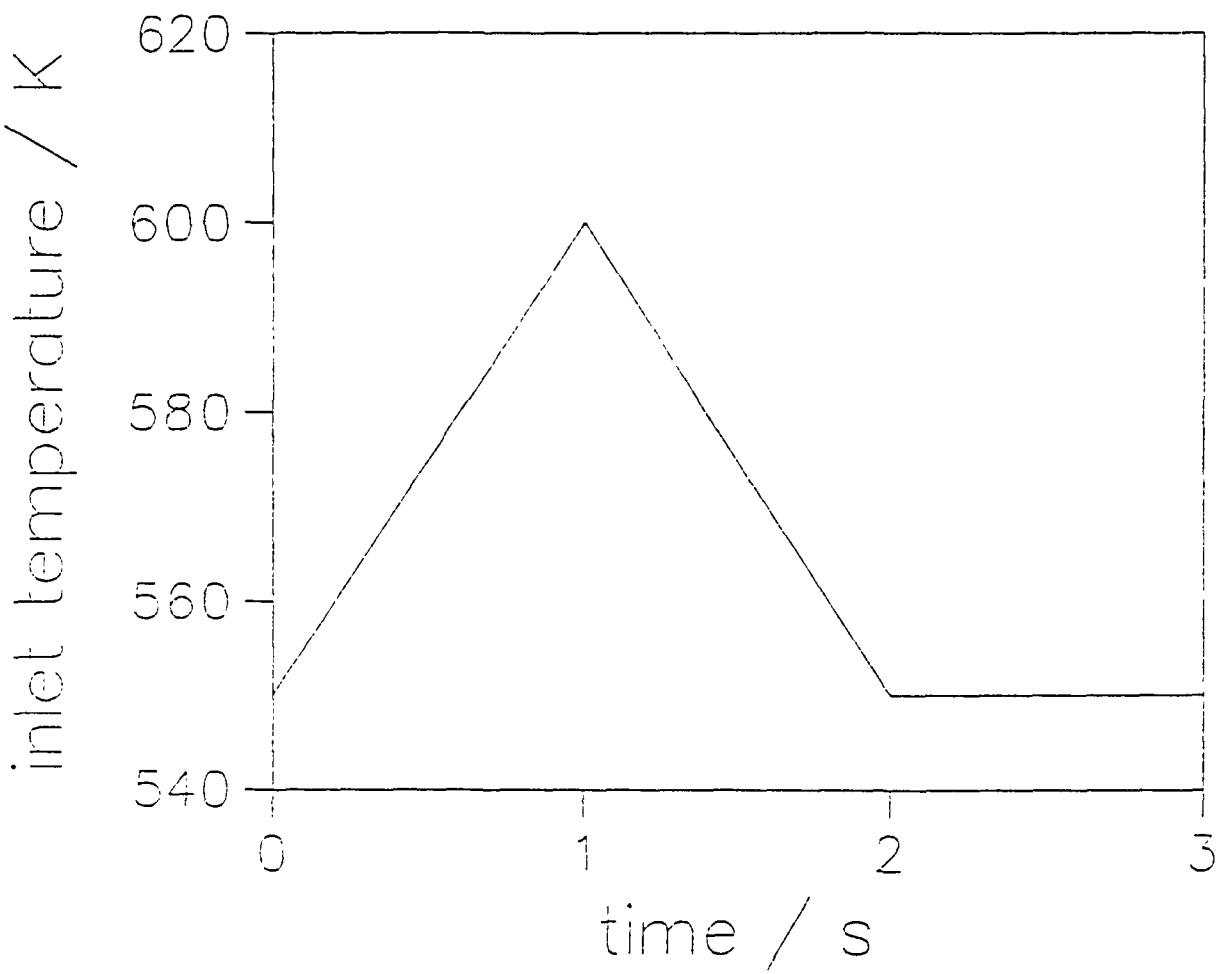

Figure 9

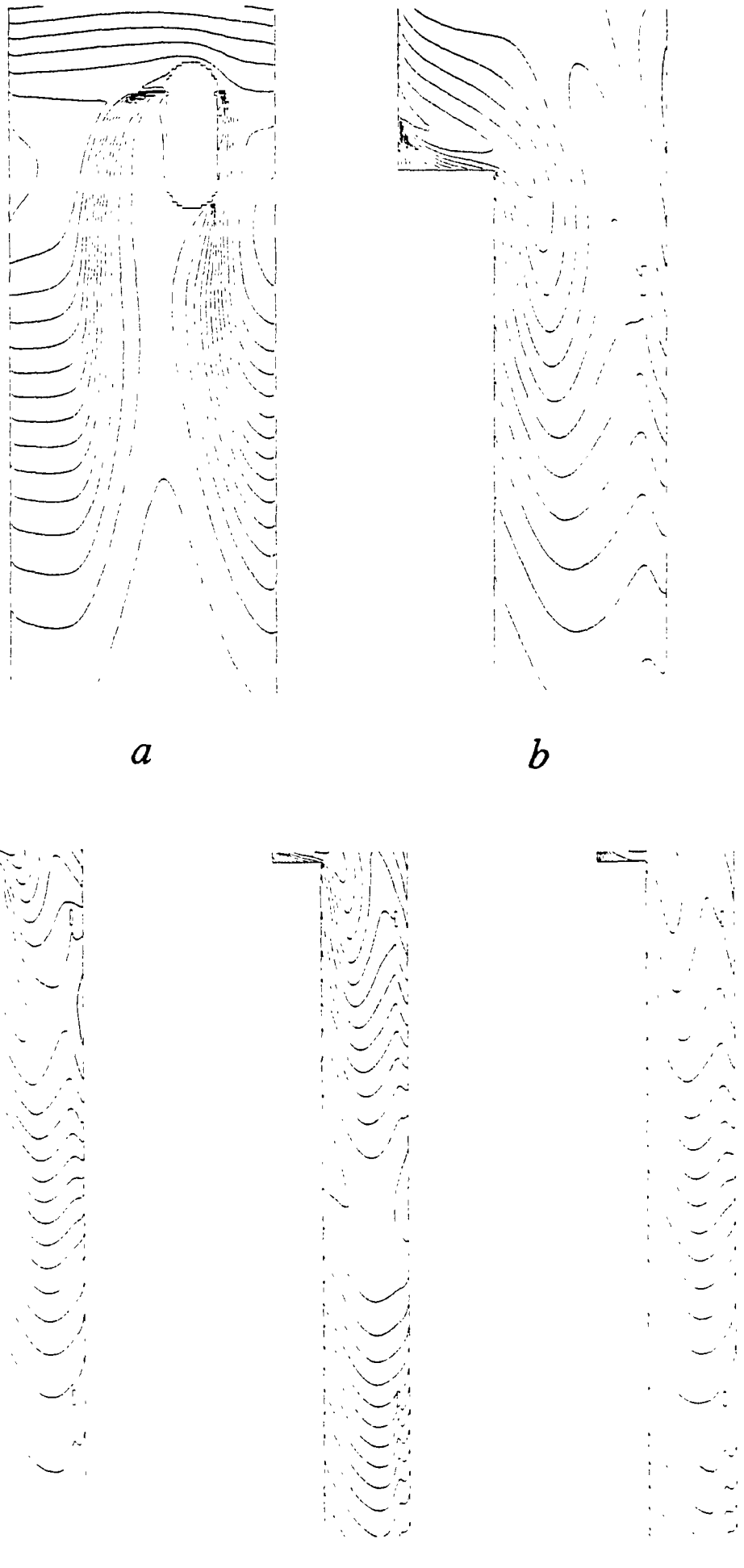

Figure 10

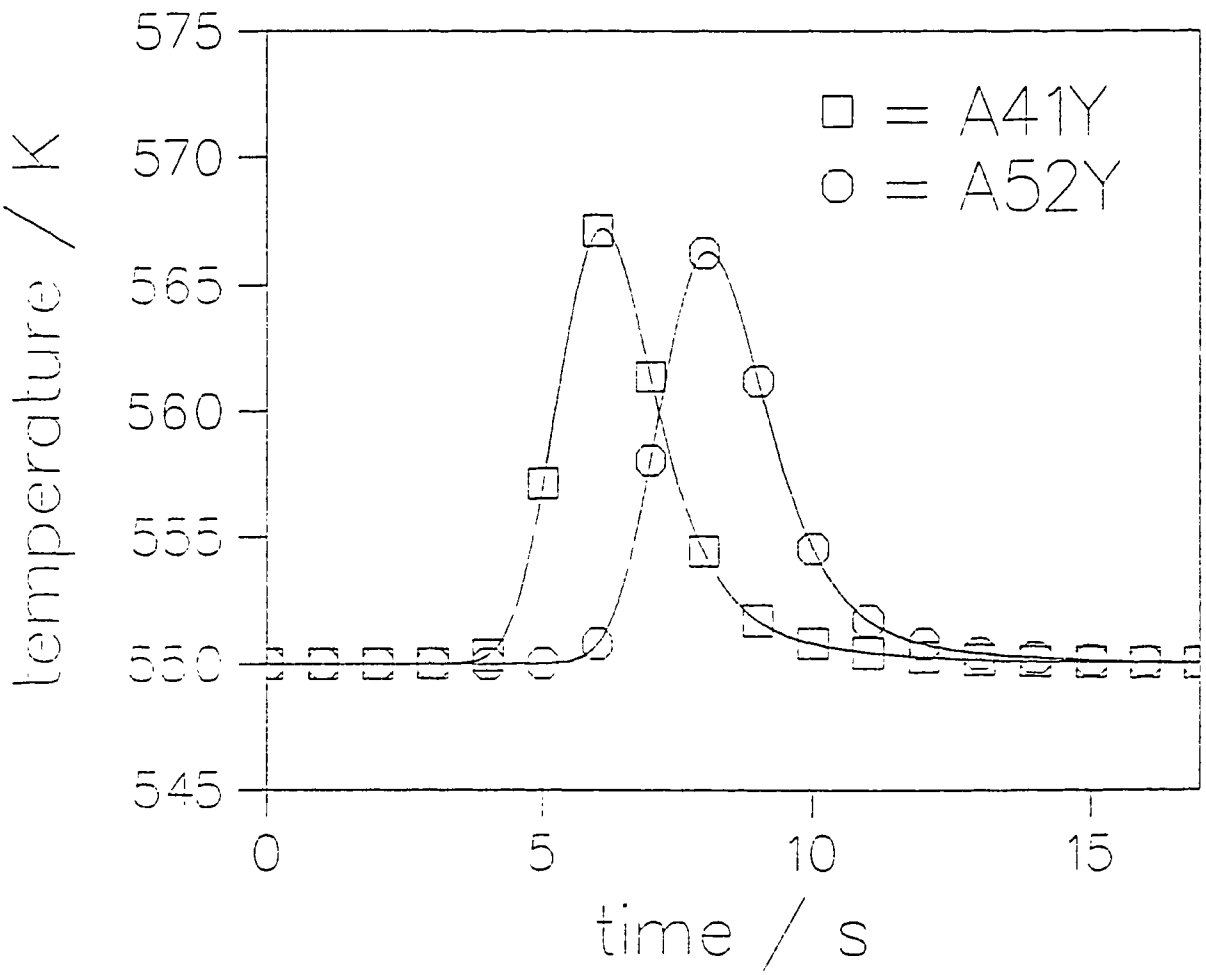
575
570
565
560
555
550
545
temperature / K
□ = A41Y
○ = A52Y
0
5
10
15
time / s

Figure 11

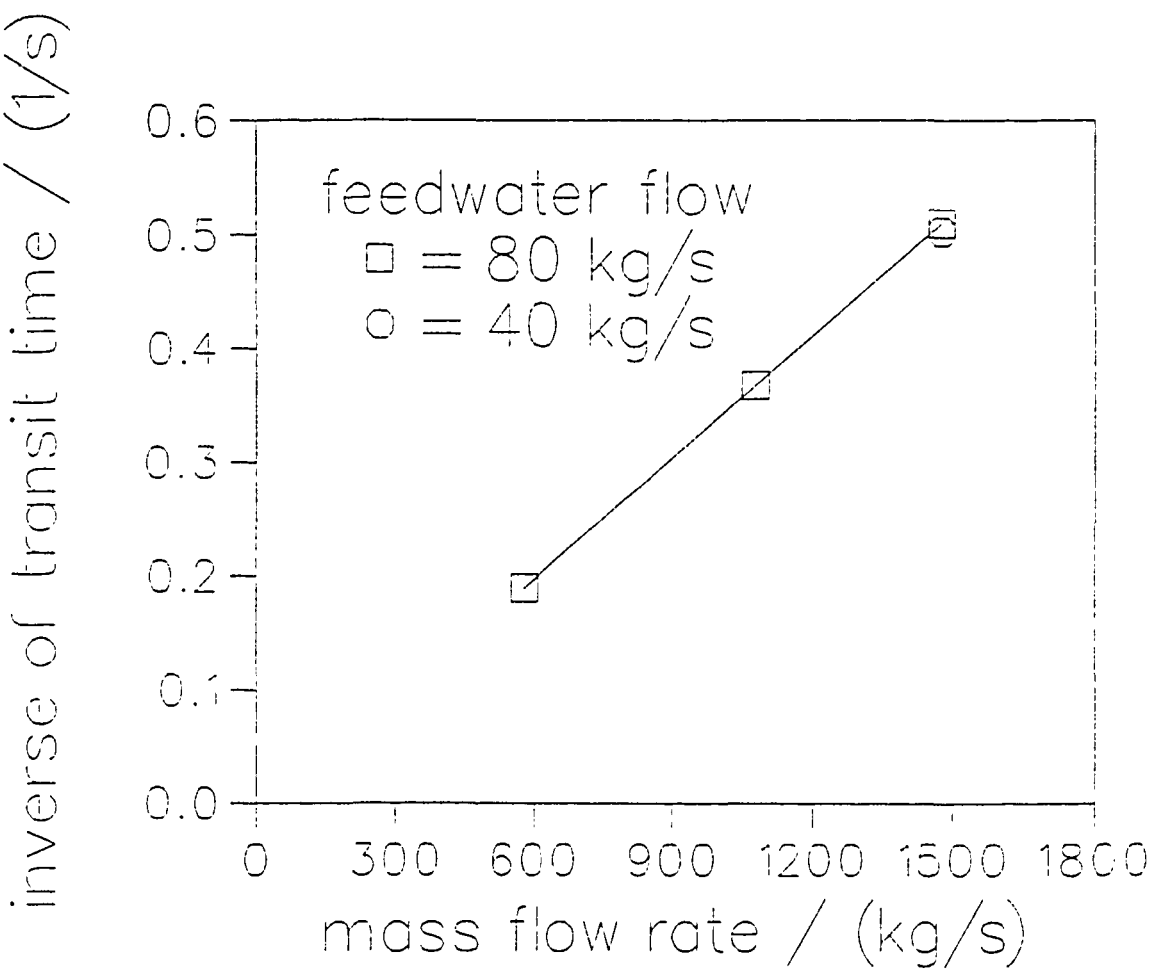
inverse of transit time / (1/s)
0.6
0.5
0.4
0.3
0.2
0.1
0.0
feedwater flow
□ = 80 kg/s
○ = 40 kg/s
0
300
600
900
1200
1500
1800
mass flow rate / (kg/s)

Figure 12

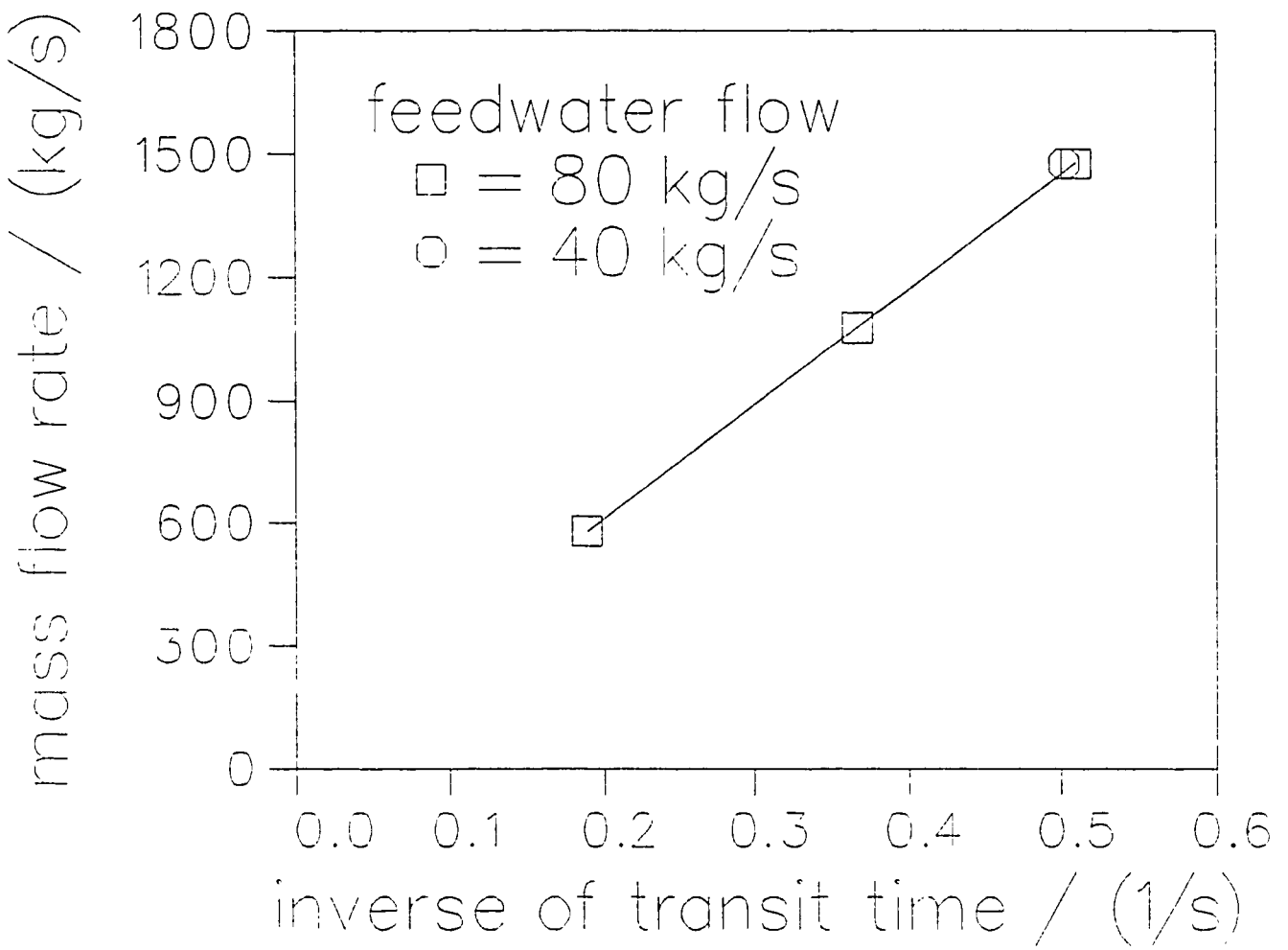
mass flow rate / (kg/s)
1800
1500
1200
900
600
300
0
feedwater flow
□ = 80 kg/s
○ = 40 kg/s
0.0
0.1
0.2
0.3
0.4
0.5
0.6
inverse of transit time / (1/s)

Figure 13